

Propagating modes of periodic solid layers in an ideal or viscous fluid by homogenization analysis

Ying-Hong Liu,¹ Chien C. Chang,^{1,2,*} and Chih-Yu Kuo¹

¹*Division of Mechanics, Research Center for Applied Sciences, Academia Sinica, Taipei, Taiwan 115, Republic of China*

²*Institute of Applied Mechanics and Taida Institute of Mathematical Sciences, National Taiwan University, Taipei, Taiwan 106, Republic of China*

(Received 14 March 2008; revised manuscript received 13 June 2008; published 20 August 2008)

This study is aimed at investigation of propagating modes of acoustic waves in periodic solid layers in ideal or viscous fluids. In particular, at the long-wavelength limit, a three-scale homogenization analysis is developed to derive the effective group velocities in analytical forms for the shear-vertical (SV) waves as well as for the longitudinal-shear-horizontal (P-SH) waves. It is found that propagating modes, i.e., modes with real group velocities, may be supported even if the fluid phase is viscous. A criterion for the existence of a vanishing effective viscosity is derived based on composite medium constants and the filling ratio of the fluid phase. The critical filling ratios at which an evanescent mode changes to a propagating mode are given for various solid-water systems.

DOI: [10.1103/PhysRevB.78.054115](https://doi.org/10.1103/PhysRevB.78.054115)

PACS number(s): 43.35.+d, 46.40.Cd, 63.20.-e

I. INTRODUCTION

Artificial solid periodic structures have attracted a great deal of interest because of the unusual properties of these materials. Recent advances in fabricating solid composites at small scale, which are either elastic or optical, pose an important question of practical interest: What effective (or global) behaviors are exhibited by the microstructures? In this study, we are concerned with acoustic waves in elastic materials.

In literature, the effective properties of elastic solid-solid composites have been studied by several authors.¹⁻⁷ These studies presented results on band structures as well as on averaged properties such as effective mass, elastic constants, and group velocities in the long-wavelength limit. In particular, Krokhn *et al.*⁸ used the pressure wave equation to derive the effective speed of sound for a periodic array of the liquid-gas mixture. They also used the elastic wave equation to derive the effective speed of the sound of the shear-vertical waves for a two-dimensional array of solid-solid structures. Subsequently, Ni and Cheng^{9,10} extended their work to include all the propagating modes for two-dimensional as well as three-dimensional periodic solid-solid structures.

Relatively fewer works have been devoted to the study of solid-fluid composite systems. Berryman^{11,12} derived a new expression of effective-mass density for all spatial dimensions, based on average T -matrix approach. Mei *et al.*¹³ were concerned with the use of the expression in applying the multiple-scattering theory to solve the full elastic wave equations. On the other hand, Sprik and Wegdam¹⁴ computed the band structure of periodic solid-viscous liquid composites. Zhang *et al.*¹⁵ studied how the viscosity helps to open the acoustic band gaps of a two-dimensional array of solid cylinders in viscous liquid. The questions then are: Can there be propagating modes when the fluid phase is subject to viscous damping? What types of modes can be supported by composite solid-fluid systems? It must be noted that although fluids cannot support propagating transverse waves, they can

support evanescent transverse waves if they have viscosity. In this study, we explore the effective properties of propagating modes in the fluid-solid system where the fluid phase is either inviscid or viscous.

In an earlier work, the present authors¹⁶ presented a two-scale homogenization analysis used to study the effects of mass density ratio and elastic constant contrast on the major band gaps of elastic periodic structures. The two scales include a fine scale and a coarse-grained scale, which differ in magnitude on the order of the ratio of the size of the periodic unit to the incident wavelength. However, the analysis cannot be applied here because of the vanishing shear modulus in the fluid phase. To overcome the difficulties, instead of treating a material property at the interface between the fluid and the solid phases as a sharp discontinuity, we approximate each material property at the interface by a continuous function which changes in a scale much smaller than the scale of the unit cell. This sharp layer is called an interfacial layer and its length scale is called an interfacial scale. A three-scale homogenization analysis based on these interfacial, coarse-grained, and fine scales is here developed to derive effective-medium properties. In Sec. III of the paper, we will develop the homogenization analysis for the solid-fluid composite layers by assuming an ideal fluid, i.e., a fluid without viscous damping. In particular, effective elastic constants and group velocities for the shear-vertical (SV) modes as well as for longitudinal-shear horizontal (P-SH) modes will be obtained in analytical forms. In Sec. IV, the fluid is considered to be viscous, and it is more convenient to develop the homogenization analysis in the frequency domain, for which we use complex Lamé constants for the fluid. The main point of interest is to explore if there is a possibility that any effective viscosity may vanish under some particular physically realizable conditions and lead to propagating modes on the coarse-grained scales.

II. BASIC EQUATIONS

Let us start with the time-dependent form of the elastic wave equation,

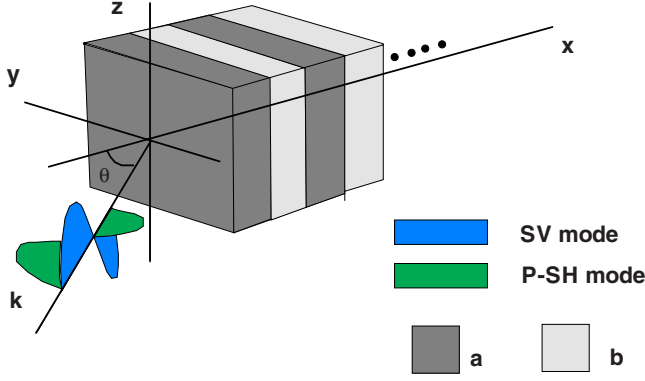


FIG. 1. (Color online) This figure depicts the distinctive modes of the incident wave that make an angle θ with the x axis on the xy plane. The SV mode is plotted in blue, where the displacement is in the z axis. The P-SH mode is plotted in green, where the displacement is on the xy plane.

$$\frac{\partial}{\partial x_j} \left(C_{ijmn} \frac{\partial u_m}{\partial x_n} \right) = \rho \frac{\partial^2 u_i}{\partial t^2}, \quad (1)$$

where u_i is the displacement, C_{ijmn} is the elastic constant, and ρ is the mass density. In order to investigate the group velocity of the composite material at the low-frequency limit for periodic structures, we apply the theory of homogenization (see, e.g., Refs. 16 and 17). Let us consider a wave propagating with a large wavelength l , i.e., $\epsilon = d/l \ll 1$, where d is the unit length of periodic layers. It is convenient to do dimensionless analysis by introducing $x_j \rightarrow dx_j$, $C_{ijmn} \rightarrow C_c C_{ijmn}$, $\rho \rightarrow \rho_c \rho$, and $t \rightarrow 2\pi t / \omega_c$, where C_c , ρ_c , and ω_c are the characteristic values of elastic constants, mass density, and frequency.^{16,17} Then we have the dimensionless elastic equation

$$\frac{\partial}{\partial x_j} \left(C_{ijmn} \frac{\partial u_m}{\partial x_n} \right) = \epsilon^2 \rho \frac{\partial^2 u_i}{\partial t^2}, \quad (2)$$

where we identify the large wavelength l such that $l^2 = 4\pi^2 C_c / \rho_c \omega_c^2$. For simplicity, we consider the periodic layer made of a fluid and a cubic material and separate the waves into the SV and P-SH modes as shown in Fig. 1. Thus Eq. (2) could be written in the SV mode as

$$\frac{\partial}{\partial x} \left(C_{44} \frac{\partial u_z}{\partial x} \right) + \frac{\partial}{\partial y} \left(C_{44} \frac{\partial u_z}{\partial y} \right) = \epsilon^2 \rho \frac{\partial^2 u_z}{\partial t^2}, \quad (3)$$

and in the P-SH mode as

$$\begin{aligned} \frac{\partial}{\partial x} \left(C_{11} \frac{\partial u_x}{\partial x} \right) + \frac{\partial}{\partial y} \left(C_{44} \frac{\partial u_x}{\partial y} \right) + \frac{\partial}{\partial x} \left(C_{12} \frac{\partial u_y}{\partial y} \right) + \frac{\partial}{\partial y} \left(C_{44} \frac{\partial u_y}{\partial x} \right) \\ = \epsilon^2 \rho \frac{\partial^2 u_x}{\partial t^2}, \end{aligned} \quad (4)$$

$$\begin{aligned} \frac{\partial}{\partial x} \left(C_{12} \frac{\partial u_x}{\partial x} \right) + \frac{\partial}{\partial x} \left(C_{44} \frac{\partial u_x}{\partial y} \right) + \frac{\partial}{\partial x} \left(C_{44} \frac{\partial u_y}{\partial x} \right) + \frac{\partial}{\partial y} \left(C_{11} \frac{\partial u_y}{\partial y} \right) \\ = \epsilon^2 \rho \frac{\partial^2 u_y}{\partial t^2}. \end{aligned} \quad (5)$$

III. HOMOGENIZATION ANALYSIS OF SOLID LAYERS IN IDEAL FLUID

In this section, we shall develop homogenization analyses for the SV mode and the P-SH mode.

A. SV mode

First, we consider the SV mode,

$$\frac{\partial}{\partial x} \left(C_{44} \frac{\partial u_z}{\partial x} \right) + \frac{\partial}{\partial y} \left(C_{44} \frac{\partial u_z}{\partial y} \right) = \epsilon^2 \rho \frac{\partial^2 u_z}{\partial t^2}, \quad (6)$$

where we note that the shear modulus $C_{44}=0$ in the fluid region. Let ϕ be the proportion of the composite occupied by the fluid phase. In order to analyze the fluid-solid system in a unified approach, we make the following approximation:

$$\bar{C}_{44} = H(x - \phi) C_{44} \rightarrow \frac{C_{44}}{1 + e^{-(x-\phi)/\epsilon}}, \quad (7)$$

where $H(x-\phi)$ is the Heaviside step function. In other words, we introduce a transition layer of order ϵ in thickness at the interface of the fluid and solid. This modification leads us to perform three-scale analysis by introducing $x=x$ (fine scale), $\bar{x}=(x-\phi)/\epsilon$ (interface scale), and $x'=\epsilon x$ (coarse-grained scale). The sound wave propagates in the coarse-grained scale. Hence the displacement u_z is considered as a function of \bar{x} , x , and x' , i.e., $u_z = u_z(\bar{x}, x, x') e^{i\beta y'}$, where β is the wave number along the y axis in the coarse-grained scale $y' = \epsilon y$. Then, the derivative with respect to x becomes

$$\frac{\partial}{\partial x} \rightarrow \frac{1}{\epsilon} \frac{\partial}{\partial \bar{x}} + \frac{\partial}{\partial x} + \epsilon \frac{\partial}{\partial x'} = \frac{D_x}{\epsilon}. \quad (8)$$

The perturbation analysis follows the standard approach: expanding u_z in powers of ϵ , $u_z = u_z^0 + \epsilon u_z^1 + \epsilon^2 u_z^2 + \dots$; substituting these expressions into Eq. (6); and collecting terms of like powers in ϵ from the zeroth to the fourth order. After replacing the x and u_z of perturbation terms, Eq. (6) becomes

$$\begin{aligned} D_x [\bar{C}_{44} D_x (u_z^0 + \epsilon u_z^1 + \epsilon^2 u_z^2 + \dots)] \\ - \epsilon^4 \beta^2 \bar{C}_{44} (u_z^0 + \epsilon u_z^1 + \epsilon^2 u_z^2 + \dots) \\ = \epsilon^4 \rho \frac{\partial^2 u_z^0}{\partial t^2} + \dots \end{aligned} \quad (9)$$

Next we collect terms of each power in ϵ from zeroth to fourth order. For the order $O(\epsilon^0)$, we get

$$\frac{\partial}{\partial \bar{x}} \left(\bar{C}_{44} \frac{\partial u_z^0}{\partial \bar{x}} \right) = 0, \quad (10)$$

where u_z^0 denotes the coarse-grained displacement; it cannot depend on \bar{x} if periodic conditions are considered. For the orders $O(\epsilon^1)$ and $O(\epsilon^2)$, we have

$$\frac{\partial}{\partial \bar{x}} \left[\bar{C}_{44} \left(\frac{\partial u_z^1}{\partial \bar{x}} + \frac{\partial u_z^0}{\partial x'} \right) \right] = 0, \quad (11)$$

$$\frac{\partial}{\partial \bar{x}} \left[\bar{C}_{44} \left(\frac{\partial u_z^2}{\partial \bar{x}} + \frac{\partial u_z^1}{\partial x} + \frac{\partial u_z^0}{\partial x'} \right) \right] = 0. \quad (12)$$

A general solution of u_z^2 can be expressed in the form

$$u_z^2 = Q_1(\bar{x}, x, x') \left(\frac{\partial u_z^0}{\partial x'} + \frac{\partial u_z^1}{\partial x} \right) + \bar{u}_z^2(x, x'), \quad (13)$$

where $Q_1(\bar{x}, x, x')$ is a periodic function in x of period 1 and $\bar{u}_z^2(x')$ is independent of \bar{x} . Substituting u_z^2 of Eq. (13) into Eq. (12), we obtain

$$\frac{\partial}{\partial \bar{x}} \left[\bar{C}_{44} \left(1 + \frac{\partial Q_1}{\partial \bar{x}} \right) \right] = 0. \quad (14)$$

A simple integration gives

$$Q_1 = -(\bar{x} + \bar{\phi}) + D_1 \int_{-\bar{\phi}}^{\bar{x}} \frac{ds}{\bar{C}_{44}} + D_2, \quad (15)$$

where $\bar{\phi}$ is measured on the scale of $\Delta = 1/\epsilon$, i.e., $\bar{\phi} = \phi\Delta$. (A similar procedure of homogenization can be found in Ref. 16.) D_1 and D_2 are functions of x and x' only. Since Q_1 must be a periodic function of x with period 1, D_1 can be depicted by leading behavior,

$$D_1 = C_{44}^e = \frac{\Delta C_{44}}{\Delta - e^{-\Delta + \bar{\phi}} - e^{\bar{\phi}}} \approx \begin{cases} C_{44} \phi^{-1} e^{-\Delta}, & \phi \neq 0, \quad \Delta \rightarrow \infty \\ C_{44}, & \phi = 0, \quad \Delta \rightarrow \infty, \end{cases} \quad (16)$$

and D_2 can simply be taken as zero. Comparing to the conventional two-scale analysis applied to solid-solid systems, D_1 is determined by an integral of $1/C_{44}$. One faces the problem of not being able to integrate over the liquid phase. On the contrary, by introducing the interface layer, we can carry out the wavelength of D_1 . In the next order of analysis, $O(\epsilon^3)$, we can see that D_1 is in fact the effective elastic constant of C_{44} on the coarse-grained scale. An intriguing property is that the effective elastic constant D_1 decreases to zero no matter how thin the fluid phase exists in the structural array.

For $O(\epsilon^3)$, we get

$$\frac{\partial}{\partial \bar{x}} \left[\bar{C}_{44} \left(\frac{\partial u_z^2}{\partial \bar{x}} + \frac{\partial u_z^1}{\partial x} \right) \right] + \frac{\partial}{\partial x} \left[C_{44}^e \left(\frac{\partial u_z^1}{\partial x} + \frac{\partial u_z^0}{\partial x'} \right) \right] = 0. \quad (17)$$

The equation has no effect on the next-order analysis and will not be pursued further. For $O(\epsilon^4)$, we get

$$\begin{aligned} & \frac{\partial}{\partial \bar{x}} \left[\bar{C}_{44} \frac{\partial u_z^2}{\partial \bar{x}} \right] + \frac{\partial}{\partial x} \left[\bar{C}_{44} \left(\frac{\partial u_z^2}{\partial x} + \frac{\partial u_z^1}{\partial x'} \right) \right] \\ & + \frac{\partial}{\partial x'} \left[\bar{C}_{44} \left(\frac{\partial u_z^2}{\partial \bar{x}} + \frac{\partial u_z^1}{\partial x} + \frac{\partial u_z^0}{\partial x'} \right) \right] - \beta^2 \bar{C}_{44} u_z^0 = \rho \frac{\partial^2}{\partial t^2} u_z^0. \end{aligned} \quad (18)$$

For waves in the coarse-grained scale, we take the average of Eq. (18) over a unit scale. The first and second terms after

being averaged with respect to x become zero because of the periodic boundary conditions. Finally, it is found by using the current homogenization analysis that u_z^0 is a function dependent only on the coarse-grained variable x' and satisfies the averaged equation

$$\frac{\partial}{\partial x'} \left(C_{44}^e \frac{\partial u_z^0}{\partial x'} \right) - \beta^2 \langle C_{44} \rangle u_z^0 = \langle \rho \rangle \frac{\partial^2 u_z^0}{\partial t^2}, \quad (19)$$

where $\langle \dots \rangle$ denotes the volume average over one unit cell. In this equation, $\langle C_{44} \rangle = (1 - \phi)C_{44}$ and $\langle \rho \rangle = \phi\rho_f + (1 - \phi)\rho_s$, where ρ_s and ρ_f are the mass densities of the solid and the fluid, respectively. The effective group velocity in the coarse-grained scale, $v_{g,SV}$ of the SV mode with an arbitrary direction of incident wave can be found straightforwardly,

$$v_{g,SV}^2 = \left(\frac{\partial \omega}{\partial k} \right)_{\omega, k \rightarrow 0}^2 = \frac{C_{SV}^e}{\langle \rho \rangle} = \frac{\cos^2 \theta C_{44}^e + \sin^2 \theta \langle C_{44} \rangle}{\langle \rho \rangle}. \quad (20)$$

B. P-SH mode

Next we consider the P-SH mode. The elastic constants with the interface layer approach are

$$\bar{C}_{11} = C_{11}^s / (1 + e^{-(x-\phi)/\epsilon}) + C_{11}^f / (1 + e^{(x-\phi)/\epsilon}), \quad (21)$$

$$\bar{C}_{12} = C_{12}^s / (1 + e^{-(x-\phi)/\epsilon}) + C_{12}^f / (1 + e^{(x-\phi)/\epsilon}), \quad (22)$$

where C^s and C^f denote the elastic constants for the portion of the solid and fluid, respectively. Following the same three-scale analysis, we get

$$\begin{aligned} & D_x [\bar{C}_{11} D_x (u_x^0 + \epsilon u_x^1 + \epsilon^2 u_x^2 + \dots)] \\ & - \epsilon^4 \beta^2 \bar{C}_{44} (u_x^0 + \epsilon u_x^1 + \epsilon^2 u_x^2 + \dots) \\ & + i \epsilon^2 \beta D_x [\bar{C}_{12} (u_y^0 + \epsilon u_y^1 + \epsilon^2 u_y^2 + \dots)] \\ & + \bar{C}_{44} D_x (u_y^0 + \epsilon u_y^1 + \epsilon^2 u_y^2 + \dots)] \\ & = \epsilon^4 \rho \frac{\partial^2 u_x^0}{\partial t^2} + \dots \end{aligned} \quad (23)$$

and

$$\begin{aligned} & D_x [\bar{C}_{44} D_x (u_y^0 + \epsilon u_y^1 + \epsilon^2 u_y^2 + \dots)] \\ & - \epsilon^4 \beta^2 \bar{C}_{11} (u_y^0 + \epsilon u_y^1 + \epsilon^2 u_y^2 + \dots) \\ & + i \epsilon^2 \beta D_x [\bar{C}_{44} (u_x^0 + \epsilon u_x^1 + \epsilon^2 u_x^2 + \dots)] \\ & + \bar{C}_{12} D_x (u_x^0 + \epsilon u_x^1 + \epsilon^2 u_x^2 + \dots)] \\ & = \epsilon^4 \rho \frac{\partial^2 u_y^0}{\partial t^2} + \dots \end{aligned} \quad (24)$$

From the experience of the SV mode, the zeroth order of the displacements presents in the macroscale that the layered structure could be treated as homogeneous medium. This idea enables us to assume that u_x^0 and u_y^0 depend only on x' . In addition, u_x^1 and u_y^1 are the functions of x and x' . For $O(\epsilon^2)$, we get

$$\frac{\partial}{\partial \bar{x}} \left[\bar{C}_{11} \left(\frac{\partial u_x^0}{\partial x'} + \frac{\partial u_x^1}{\partial x} + \frac{\partial u_x^2}{\partial \bar{x}} \right) \right] + i\beta \frac{\partial \bar{C}_{12}}{\partial \bar{x}} u_y^0 = 0, \quad (25)$$

$$\frac{\partial}{\partial \bar{x}} \left[\bar{C}_{44} \left(\frac{\partial u_y^0}{\partial x'} + \frac{\partial u_y^1}{\partial x} + \frac{\partial u_y^2}{\partial \bar{x}} \right) \right] + i\beta \frac{\partial \bar{C}_{44}}{\partial \bar{x}} u_x^0 = 0. \quad (26)$$

From Eqs. (25) and (26), we can guess the second order of the displacements induced by those from the zeroth and the first orders, in the form of

$$u_x^2 = P_1(\bar{x}, x, x') \left(\frac{\partial u_x^0}{\partial x'} + \frac{\partial u_x^1}{\partial x} \right) + P_2(\bar{x}, x, x') u_y^0 + \bar{u}_x^1(x'), \quad (27)$$

$$u_y^2 = P_3(\bar{x}, x, x') \left(\frac{\partial u_y^0}{\partial x'} + \frac{\partial u_y^1}{\partial x} \right) + P_4(\bar{x}, x, x') u_x^0 + \bar{u}_y^1(x'). \quad (28)$$

By this approach, the P and SH modes can be decoupled if $\beta=0$. Under such condition, the effective-mass density and elastic constants follow the same formulation as the SV mode. However, if β is not equal to zero, the P-SH mode is still coupled and some interesting phenomena can be uncovered using our three-scale analysis. Substituting Eqs. (27) and (28) into Eqs. (25) and (26), we rearrange the governing equations for the coefficients P ,

$$\frac{\partial}{\partial x} \left[\bar{C}_{11} \left(1 + \frac{\partial P_1}{\partial x} \right) \right] = 0, \quad (29)$$

$$\frac{\partial}{\partial x} \left[\bar{C}_{11} \frac{\partial P_2}{\partial x} + i\beta \bar{C}_{12} \right] = 0, \quad (30)$$

$$\frac{\partial}{\partial x} \left[\bar{C}_{44} \left(1 + \frac{\partial P_3}{\partial x} \right) \right] = 0, \quad (31)$$

$$\frac{\partial}{\partial x} \left[\bar{C}_{44} \frac{\partial P_4}{\partial x} + i\beta \bar{C}_{44} \right] = 0. \quad (32)$$

Integrating these equations, we obtain

$$P_1 = -(\bar{x} + \bar{\phi}) + D_{11} \int_{\bar{\phi}}^{\bar{x}} \frac{ds}{\bar{C}_{11}} + D_{12}, \quad (33)$$

$$P_2 = -i\beta \int_{\bar{\phi}}^{\bar{x}} \frac{\bar{C}_{12}}{\bar{C}_{11}} ds + D_{21} \int_{\bar{\phi}}^{\bar{x}} \frac{ds}{\bar{C}_{11}} + D_{22}, \quad (34)$$

$$P_3 = -(\bar{x} + \bar{\phi}) + D_{31} \int_{\bar{\phi}}^{\bar{x}} \frac{ds}{\bar{C}_{44}} + D_{32}, \quad (35)$$

$$P_4 = -i\beta(\bar{x} + \bar{\phi}) + D_{41} \int_{\bar{\phi}}^{\bar{x}} \frac{ds}{\bar{C}_{44}} + D_{42}, \quad (36)$$

where

$$\begin{aligned} D_{11} &= \frac{C_{11}^s C_{11}^f / \epsilon}{C_{11}^s / \epsilon + (C_{11}^f - C_{11}^s) \log \left(\frac{e^{(1-\phi)/\epsilon} C_{11}^s + C_{11}^f}{e^{-\phi/\epsilon} C_{11}^s + C_{11}^f} \right)} \\ &\approx \frac{C_{11}^s C_{11}^f}{(1-\phi) C_{11}^f + \phi C_{11}^s} \\ &= \left\langle \frac{1}{C_{11}} \right\rangle^{-1} = C_{11}^e, \end{aligned} \quad (37)$$

$$D_{21} \approx \frac{i\beta}{\left\langle \frac{1}{C_{11}} \right\rangle} \left[\phi \frac{C_{12}^f}{C_{11}^f} + (1-\phi) \frac{C_{12}^s}{C_{11}^s} \right] = i\beta C_{11}^e \left\langle \frac{C_{12}}{C_{11}} \right\rangle, \quad (38)$$

$$D_{31} = \frac{D_{41}}{i\beta} = D_1 = C_{44}^e. \quad (39)$$

Here C_{11}^e denotes the harmonic mean for C_{11} of the materials. For the $O(\epsilon^3)$, we have

$$\begin{aligned} \frac{\partial}{\partial \bar{x}} \left[\bar{C}_{11} \left(\frac{\partial u_x^2}{\partial x} + \frac{\partial u_x^1}{\partial x'} \right) + i\beta \frac{\partial}{\partial \bar{x}} (\bar{C}_{12} u_y^1) \right] \\ + \frac{\partial}{\partial x} \left[D_{11} \left(\frac{\partial u_x^1}{\partial x} + \frac{\partial u_x^0}{\partial x'} \right) \right] + \frac{\partial D_{21}}{\partial x} u_y^0 = 0 \end{aligned} \quad (40)$$

and

$$\begin{aligned} \frac{\partial}{\partial \bar{x}} \left[\bar{C}_{44} \left(\frac{\partial u_y^2}{\partial x} + \frac{\partial u_y^1}{\partial x'} \right) + i\beta \frac{\partial}{\partial \bar{x}} (\bar{C}_{44} u_x^1) \right] \\ + \frac{\partial}{\partial x} \left[D_{31} \left(\frac{\partial u_y^1}{\partial x} + \frac{\partial u_y^0}{\partial x'} \right) \right] + \frac{\partial D_{41}}{\partial x} u_x^0 = 0. \end{aligned} \quad (41)$$

These equations have no effect on the next-order analysis and will not be pursued further based on the same reasoning as in the SV mode. Finally, for the $O(\epsilon^4)$, we have

$$\begin{aligned} \frac{\partial}{\partial \bar{x}} \left(\bar{C}_{11} \frac{\partial u_x^2}{\partial x'} \right) + \frac{\partial}{\partial x} \left[\bar{C}_{11} \left(\frac{\partial u_x^2}{\partial x} + \frac{\partial u_x^1}{\partial x'} \right) \right] + i\beta \frac{\partial}{\partial \bar{x}} (\bar{C}_{12} u_y^2) \\ + i\beta \left[\frac{\partial}{\partial x} (\bar{C}_{12} u_y^1) + \frac{\partial}{\partial x'} (\bar{C}_{12} u_y^0) \right] \\ + \bar{C}_{44} \left(\frac{\partial u_y^2}{\partial \bar{x}} + \frac{\partial u_y^1}{\partial x} + \frac{\partial u_y^0}{\partial x'} \right) \\ + \frac{\partial}{\partial x'} \left[\bar{C}_{11} \left(\frac{\partial u_x^2}{\partial \bar{x}} + \frac{\partial u_x^1}{\partial x} + \frac{\partial u_x^0}{\partial x'} \right) \right] - \beta^2 C_{44} u_x^0 \\ = \rho \frac{\partial^2 u_x^0}{\partial t^2} \end{aligned} \quad (42)$$

and

$$\begin{aligned}
 & \frac{\partial}{\partial \bar{x}} \left(\bar{C}_{44} \frac{\partial u_y^2}{\partial x'} \right) + \frac{\partial}{\partial x} \left[\bar{C}_{44} \left(\frac{\partial u_y^2}{\partial x} + \frac{\partial u_y^1}{\partial x'} \right) \right] + i\beta \frac{\partial}{\partial \bar{x}} (\bar{C}_{44} u_x^2) \\
 & + i\beta \left[\frac{\partial}{\partial x} (\bar{C}_{44} u_x^1) + \frac{\partial}{\partial x'} (\bar{C}_{44} u_x^0) \right. \\
 & \left. + \bar{C}_{12} \left(\frac{\partial u_x^2}{\partial \bar{x}} + \frac{\partial u_x^1}{\partial x} + \frac{\partial u_x^0}{\partial x'} \right) \right] \\
 & + \frac{\partial}{\partial x'} \left[\bar{C}_{44} \left(\frac{\partial u_y^2}{\partial \bar{x}} + \frac{\partial u_y^1}{\partial x} + \frac{\partial u_y^0}{\partial x'} \right) \right] - \beta^2 C_{11} u_y^0 \\
 & = \rho \frac{\partial^2 u_y^0}{\partial t^2}. \tag{43}
 \end{aligned}$$

In order to see the behavior on the macroscale, we take the average of Eqs. (42) and (43) over the unit cell. The terms of the surface integrals with respect to x vanish because of the periodic boundary conditions. The resulting equations are

$$\frac{\partial}{\partial x'} \left(C_{11}^e \frac{\partial u_x^0}{\partial x'} \right) + i\beta P \frac{\partial u_y^0}{\partial x'} - \beta^2 C_{44}^e u_x^0 = \langle \rho \rangle \frac{\partial^2 u_x^0}{\partial t^2}, \tag{44}$$

$$\frac{\partial}{\partial x'} \left(C_{44}^e \frac{\partial u_y^0}{\partial x'} \right) + i\beta Q \frac{\partial u_x^0}{\partial x'} - \beta^2 Q u_y^0 = \langle \rho \rangle \frac{\partial^2 u_y^0}{\partial t^2}. \tag{45}$$

For a nontrivial solution to exist, we have the dispersion relation

$$\begin{bmatrix} -\omega^2 \langle \rho \rangle + Rk^2 & Pk^2 \cos \theta \sin \theta \\ Pk^2 \cos \theta \sin \theta & -\omega^2 \langle \rho \rangle + Sk^2 \end{bmatrix} = 0. \tag{46}$$

In the above equations, we have defined $P = C_{11}^e \langle \frac{C_{12}}{C_{11}} \rangle + C_{44}^e$, $R = C_{11}^e \cos^2 \theta + C_{44}^e \sin^2 \theta$, and $S = C_{44}^e \cos^2 \theta + Q \sin^2 \theta$, where $Q = -\langle \frac{C_{12}^2}{C_{11}} \rangle + \langle C_{11} \rangle + C_{11}^e \langle \frac{C_{12}}{C_{11}} \rangle^2$. The effective group velocities, $v_{g,SH}$ and $v_{g,P}$, of the P-SH mode are hence

$$v_{g,SH}^2 = \frac{C_{SH}^e}{\langle \rho \rangle} = \frac{(R+S) - \sqrt{(R-S)^2 + 4P^2 \cos^2 \theta \sin^2 \theta}}{2\langle \rho \rangle}, \tag{47}$$

$$v_{g,P}^2 = \frac{C_P^e}{\langle \rho \rangle} = \frac{(R+S) + \sqrt{(R-S)^2 + 4P^2 \cos^2 \theta \sin^2 \theta}}{2\langle \rho \rangle}, \tag{48}$$

where C_{SH}^e denotes the corresponding effective shear modulus of the SH mode and C_P^e is the P one.

As an example, we consider the Pb-water system, the materials of which have the physical constants shown in Table I.¹⁸ We choose three filling ratios $(1-\phi)$ for Pb: 0.2, 0.5, and 0.8. Figure 2 shows the effective velocities of the three wave modes versus the incident angle. The trend of the effective group velocity of the SV mode is from the harmonic average $C_{44}^e/\langle \rho \rangle$ to the volume average $\langle C_{44} \rangle/\langle \rho \rangle$ with increasing incident angle from zero to $\pi/2$. It is obvious that the effective group velocity of the SV mode increases monotonically from 0 at the normal incidence to its maximum at the parallel incidence. However, the behavior of the effective group velocity of the SH mode is very different from that of the SV

TABLE I. The physical parameters of the Pb-water system. The unit of the mass density is g/cm^3 , the velocity is in km/s , and the elastic constants are in 10^9 N/m^2 .

Medium	ρ	c_l	c_t	C_{11}	C_{44}	C_{12}
Pb	11.4	2.16	0.861	53.2	8.44	36.3
Water	1.0	1.49	0.0	2.22	0.0	2.22

mode. At $\theta=0$ and $\pi/2$, the effective group velocity $v_{g,SH}$ would approach zero, which indicates that the prohibitive effect of the fluid occurs not only at $\theta=0$ but also at $\theta=\pi/2$. One remarkable difference between the SV and SH modes at $\theta=\pi/2$ is that the polarization vector of the SH mode is perpendicular to the layers, while that of the SV mode is parallel to the layers. If either of the incident direction and the polarization vector is perpendicular to the layers, the group velocity of the shear mode would be zero. In Sec. IV, we will further verify the vanishing group velocity of the SH mode at $\theta=\pi/2$ by numerical simulations of the full elastic wave equations. Next, we observe that the effective group velocity $v_{g,P}$ for the P mode comes from the harmonic average $C_{11}^e/\langle \rho \rangle$ at $\theta=0$ but reaches the value $Q/\langle \rho \rangle$ at $\theta=\pi/2$, at which Q is a combination of different volume averages of elastic constants. The effective group velocity of the P mode at smaller incident angles is kept nearly constant and then increases significantly to its maximum at the parallel incidence. Although not directly related, an analogy of this phenomenon can be found in Ref. 14. We see that the shear modes of the band structure disappear as long as the region of the inviscid fluid is connected. It shows the same behavior with our case at $\theta=0$, in which the fluid is connected. Therefore, the SV and SH modes are not allowed to propagate in the x direction.

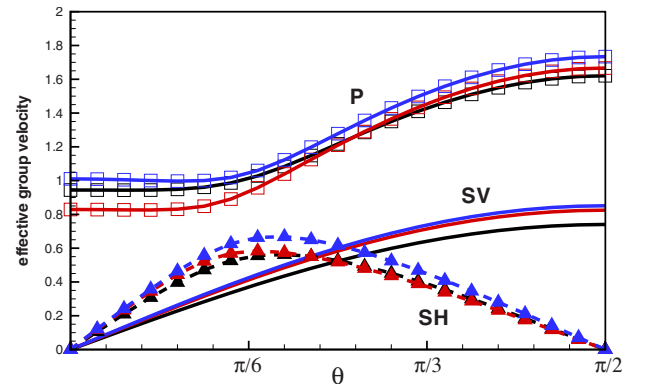


FIG. 2. (Color online) The relation between the effective group velocities of the SV, SH, and P modes and the incident angle θ . The black lines are for the filling ratios $1-\phi=0.2$ for Pb. The red lines are for 0.5 and the blue lines for 0.8. The solid lines represent the velocities of the SV mode, the dashed lines with full triangles are the velocities of the SH mode, and the solid lines with empty squares are the velocities of the P mode.

TABLE II. The physical parameters of the fluid-solid system with damping. The parameters C are the speeds of the longitudinal mode of water (Refs. 14 and 19).

Medium	ρ	C_{11}	C_{44}	C_{12}
Solid	ρ_s	C_{11}^s	C_{44}^s	C_{12}^s
Fluid	ρ_f	$\rho_f C^2 - 4i\omega\eta/3$	$-i\omega\eta$	$\rho_f C^2 + 2i\omega\eta/3$

IV. HOMOGENIZATION ANALYSIS OF SOLID LAYERS IN VISCOUS FLUID

A. SV mode

Next, we consider viscous damping in the fluid phase. Since the analysis is performed in the frequency domain, we use complex Lamé constants whose imaginary parts are associated with the material damping and are usually linearly proportional to the frequency. The solid-fluid system considered here has the physical parameters listed in Table II.^{14,19} At higher frequencies, say, on the order of 1 GHz, the corresponding wavelength is about a few micrometers. If the thickness of the periodic unit is on the order of tens or hundreds of nanometers, the above analysis is still valid. Because of damping, the pure fluid phase cannot support propagating modes. However, here we will show that propagating modes may exist for the layered fluid-solid composites if the fluid is viscous.

Let us consider the SV mode first. Our homogenization is performed for the coarse-grained scale, which equivalently corresponds to the low-frequency limit. The scaling factor is also ϵ and, hence, we can nondimensionalize C_{44} by replacing $\omega \rightarrow \epsilon\omega$:

$$C_{44} \rightarrow \frac{C_{44}^s}{1 + e^{-(x-\phi)/\epsilon}} + \frac{-i\epsilon\omega\eta}{1 + e^{(x-\phi)/\epsilon}}, \quad (49)$$

where η is the viscosity of the fluid. The perturbation analysis now needs to be carried out up to $O(\epsilon^5)$ to identify the damping effect. Substituting Eq. (49) into Eq. (6) and following the formal procedure of the three-scale homogenization analysis, we have

$$\begin{aligned} & \frac{\partial}{\partial x} \left(\frac{C_{44}^s}{1 + e^{-\bar{x}}} \frac{\partial u_z^2}{\partial x'} \right) + \frac{\partial}{\partial x'} \left[\frac{C_{44}^s}{1 + e^{-\bar{x}}} \left(\frac{\partial u_z^2}{\partial x} + \frac{\partial u_z^1}{\partial x'} \right) \right] \\ & + \frac{\partial}{\partial \bar{x}} \left(\frac{-\omega\eta i}{1 + e^{\bar{x}}} \frac{\partial u_z^2}{\partial x'} \right) + \frac{\partial}{\partial x} \left[\frac{-\omega\eta i}{1 + e^{\bar{x}}} \left(\frac{\partial u_z^2}{\partial x} + \frac{\partial u_z^1}{\partial x'} \right) \right] \\ & + \frac{\partial}{\partial x'} \left[\frac{-\omega\eta i}{1 + e^{\bar{x}}} \left(\frac{\partial u_z^2}{\partial \bar{x}} + \frac{\partial u_z^1}{\partial x} + \frac{\partial u_z^0}{\partial x'} \right) \right] \\ & + \beta^2 \frac{\omega\eta i}{1 + e^{\bar{x}}} u_z^0 - \beta^2 \frac{C_{44}^s}{1 + e^{-\bar{x}}} u_z^1 \\ & = -\rho\omega^2 u_z^1. \end{aligned} \quad (50)$$

Taking the volume integral of this equation over the unit cell with the periodic boundary conditions yields

$$\frac{\partial}{\partial x'} (-i\omega\langle\eta\rangle_{x'}) \frac{\partial u_z^0}{\partial x'} + \beta^2 (i\omega\langle\eta\rangle_{y'}) u_z^0 = D u_z^1, \quad (51)$$

where $\langle\eta\rangle_{y'} = \phi\eta$ and

$$\langle\eta\rangle_{x'} = \lim_{\epsilon \rightarrow 0} \frac{\eta C_{44}^e}{C_{44}^s} \int_0^1 \frac{1 + e^{-\bar{x}}}{1 + e^{\bar{x}}} dx = \eta. \quad (52)$$

The averaging process yields two effective viscosities $\langle\eta\rangle_{x'}$ and $\langle\eta\rangle_{y'}$. In Eq. (51), D is the operator used to modify the effective elastic constants on the fifth order but not the effective viscosity. According to the present three-scale analysis, the effective properties in the coarse-grained scale are obtained by inspecting the governing equations of $O(\epsilon^4)$ and $O(\epsilon^5)$, where the former describes the spatial wave propagation and the latter depicts the damping rate. Take note that the equation of $O(\epsilon^4)$ is the same as Eq. (19).

It is now convenient to unify the two equations to obtain the effective elastic constants with their proper effective damping rates. This is done by collecting the material coefficients after adding up the equations of these two orders. This yields the elastic constants. From Eqs. (19) and (51), we can define the effective elastic constants with damping in the macroscale as

$$\langle C_{44} \rangle_{x',x'} = C_{44}^e - i\omega\langle\eta\rangle_{x'} = C_{44}^e - i\omega\eta, \quad (53)$$

$$\langle C_{44} \rangle_{y',y'} = \langle C_{44} \rangle - i\omega\langle\eta\rangle_{y'} = \langle C_{44} \rangle - i\omega\phi\eta. \quad (54)$$

The results have two interesting consequences. Equation (53) states that once the filling ratio of the fluid is nonzero, the effective complex C_{44} in the x direction is identical to that of the fluid, as we recall from Eq. (16) that the real part C_{44}^e will go to zero when we take the limit of vanishing interfacial scale. On the other hand, Eq. (54) states that the effective complex C_{44} in the y direction has the real part $\langle C_{44} \rangle$, which modifies the C_{44} of the solid by $(1-\phi)$, and an imaginary part, which modifies the viscosity of the fluid by the filling ratio ϕ . In other words, any waves proceeding along the x direction experience a damping rate identical to that of the fluid, while the damping rate along the y direction is smaller by a factor of ϕ .

B. P-SH mode

According to the present three-scale analysis, a surprising zero effective damping is found in the P-SH modes which are presented now. As in the SV mode, we approximate the Lamé constants with the interface layer structure,

$$C_{11} \rightarrow \frac{C_{11}^s}{1 + e^{-(x-\phi)/\epsilon}} + \frac{\rho_f C^2 - \frac{4}{3}i\epsilon\omega\eta}{1 + e^{(x-\phi)/\epsilon}}, \quad (55)$$

$$C_{12} \rightarrow \frac{C_{12}^s}{1 + e^{-(x-\phi)/\epsilon}} + \frac{\rho_f C^2 + \frac{2}{3}i\epsilon\omega\eta}{1 + e^{(x-\phi)/\epsilon}}. \quad (56)$$

Carrying out the same analysis to $O(\epsilon^5)$ and volume averaging over a unit cell, we get the effective viscosity equations

$$\begin{aligned} \frac{\partial}{\partial x'} \left[(-i\omega\langle\eta\rangle_{11}) \frac{\partial u_x^0}{\partial x'} \right] + i\beta(-i\omega\langle\eta\rangle_{12}) \frac{\partial u_y^0}{\partial x'} - \beta^2(-i\omega\langle\eta\rangle_{13}) u_x^0 \\ = \bar{D}_x u_x^1 + \bar{D}_y u_y^1, \end{aligned} \quad (57)$$

$$\begin{aligned} \frac{\partial}{\partial x'} \left[(-i\omega\langle\eta\rangle_{21}) \frac{\partial u_y^0}{\partial x'} \right] + i\beta(-i\omega\langle\eta\rangle_{22}) \frac{\partial u_x^0}{\partial x'} - \beta^2(-i\omega\langle\eta\rangle_{23}) u_y^0 \\ = \hat{D}_x u_x^1 + \hat{D}_y u_y^1, \end{aligned} \quad (58)$$

where \bar{D} and \hat{D} denote the modification of effective elastic constants, not the viscosities, produced by displacements of first-order terms that we mentioned in the SV mode. The averaging process introduces six extra effective damping rates along the x and y directions. They are

$$\langle\eta\rangle_{11} = \frac{4\phi C_{11}^s \eta}{3[\phi C_{11}^s + (1-\phi)\rho_f C^2]}, \quad (59)$$

$$\langle\eta\rangle_{12} = (1-2\phi)\eta + \frac{4[\phi C_{11}^s + (1-\phi)C_{12}^s]\phi\eta}{3[\phi C_{11}^s + (1-\phi)\rho_f C^2]}, \quad (60)$$

$$\langle\eta\rangle_{13} = \langle\eta\rangle_{21} = \eta, \quad (61)$$

$$\langle\eta\rangle_{22} = \frac{\phi C_{11}^s + 3(1-\phi)\rho_f C^2}{3[\phi C_{11}^s + (1-\phi)\rho_f C^2]} \eta, \quad (62)$$

$$\langle\eta\rangle_{23} = 2\phi\eta - \frac{2[\phi C_{11}^s + (1-\phi)C_{12}^s]}{3[\phi C_{11}^s + (1-\phi)\rho_f C^2]} \phi\eta. \quad (63)$$

Hence, these equations yield the following dispersion relations if we consider that the damping effect of effective viscosities contributed to effective elastic constants only:

$$\begin{bmatrix} -\omega^2\langle\rho\rangle + R'k^2 & P'k^2 \cos\theta \sin\theta \\ P''k^2 \cos\theta \sin\theta & -\omega^2\langle\rho\rangle + S'k^2 \end{bmatrix} = 0, \quad (64)$$

where $R' = R - i\omega\langle\eta\rangle_{11} \cos^2\theta - i\omega\langle\eta\rangle_{13} \sin^2\theta$, $P' = P - i\omega\langle\eta\rangle_{12}$, $P'' = P - i\omega\langle\eta\rangle_{22}$, and $S' = S - i\omega\langle\eta\rangle_{21} \cos^2\theta - i\omega\langle\eta\rangle_{23} \sin^2\theta$. Dispersion relation (64) is identical to Eq. (46) except that P , Q , R , and S are modified as P' , Q' , R' , and S' .

As a first verification, we look at the behavior of the effective viscosities at two limiting filling ratios, say, pure liquid $\phi=1$ and solid phase with thin liquid layer $\phi=0^+$. As $\phi \rightarrow 1$, these effective viscosities reduce to those of an isotropic damping liquid smoothly. On the contrary, when $\phi \rightarrow 0^+$, $\langle\eta\rangle_{12,13,21,22}$ collapse into the nonzero value η , instead of degenerating into a pure solid case. This phenomenon is also seen in the SV mode [Eq. (53)] and, physically, represents the dramatic effects of the liquid phase to the sound wave propagation in the composite system. Another striking finding is that the viscosities $\langle\eta\rangle_{12,23}$ can possibly become zero at certain combinations of materials and filling ratios.

As an example, we consider again Pb-water system, for which $\eta=0.001$ Pa s and $\rho_f C^2=2.22 \times 10^9$ Pa.¹⁴ Figure 3 shows the effective viscosities as functions of ϕ . In this case, $\langle\eta\rangle_{23}$ goes down to zero as ϕ is decreased to 0.2179. Actu-

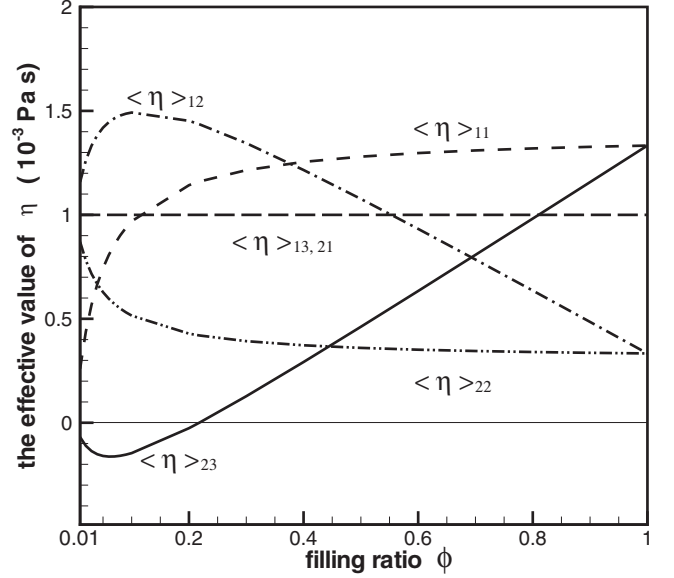


FIG. 3. The figure shows the relations of the effective η and the filling ratio for the Pb-water system with damping in the fluid phase. It is noted that there are no plots for ϕ smaller than 0.01 because a transition layer of the thickness ϵ between the solid and water is introduced. Thus ϕ cannot simply be taken as zero. Note also that $\langle\eta\rangle_{11}$ and $\langle\eta\rangle_{23}$ tend to 0, while others go to η as ϕ is decreased toward 0.

ally, from Eq. (63), $\langle\eta\rangle_{23}$ becomes negative when

$$\rho_f C^2 \leq \frac{1}{3} \left(C_{12}^s - \frac{2\phi}{1-\phi} C_{11}^s \right). \quad (65)$$

Now, the criterion in Eq. (65) raises the following question: What is the effect when $\langle\eta\rangle_{23}$ is zero? When we introduce the damping effect into the system, the frequency and wave vector could become complex variables at the same time. The experimentalists, however, typically choose one of these variables to be purely real.²⁰ Let the incident wave is driven by a source with a real frequency. Under such circumstances, the complex wave number is $k=k_1+ik_2$, such that the spatial propagating wave becomes $\exp(iky) = \exp(ik_1 y) \exp(-k_2 y)$. The effect of $\langle\eta\rangle_{23}$ appears in the pressure wave (P wave) along the y direction,

$$v_{g,P}^2|_{\theta=\pi/2} = \frac{\omega^2}{(k_1+ik_2)^2} = \frac{S'}{\langle\rho\rangle} = \frac{Q - i\omega\langle\eta\rangle_{23}}{\langle\rho\rangle}, \quad (66)$$

In the long-wavelength limit, the frequency is low and the damping is weak. Therefore, we obtain

$$k_1^2 = \frac{\langle\rho\rangle\omega^2}{Q}, \quad k_2 = \frac{\omega\langle\eta\rangle_{23}k_1}{2Q}, \quad (67)$$

where the positive branch is chosen for $+y$ to satisfy the causality condition. Now, the significance of small $\langle\eta\rangle_{23}$ is clear: The P-wave propagating mode in the y direction can be supported by the complex fluid-solid composite system. This is not seen in the case where the fluid layer is inviscid, discussed in Sec. III. This critical phenomenon is also found in a few other configurations with water liquid, which are

TABLE III. The unit of the mass density is g/cm^3 and the elastic constants are in 10^9 N/m^2 . ϕ_c is the critical value of the filling ratio at which the evanescent mode changes to a propagating one. The media are ordered from the smallest critical filling ratio to the largest. The superscript * denotes that the medium-water system does not support propagating modes.

Medium	ρ	C_{11}	C_{44}	ϕ_c
Ice	0.94	13.79	3.18	0.02716
W	19.3	500.03	151.31	0.1602
Ni	8.97	311.61	92.93	0.1604
GaAs	5.36	118.8	59.4	0.1656
C	1.75	310	88.5	0.1693
AlAs	3.76	120.2	58.9	0.1731
Ag	10.64	152.68	40.44	0.1758
Pb	11.4	53.2	8.44	0.2179
Epoxy	1.20	9.61	1.61	-0.014 25*
Rubber	1.3	6.8×10^{-4}	4.0×10^{-5}	1.0002*

listed in Table III. From this table, we find that the critical filling ratio ϕ_c is roughly located between 0.16 and 0.22 except for epoxy and rubber, whose composites with water do not support propagating modes. It must be noted that the existence of propagating modes in the solid-fluid system with viscous damping in the fluid phase is the leading-order behavior. Higher-order analysis may present damping effects, though they are at least one order smaller.

In order to support the theoretical findings by the homogenization analysis, we compute the band structures of the P-SH modes at $\theta = \pi/2$ in the low-frequency limit. The elastic wave equation for cubic materials in the frequency domain are given by

$$\frac{\partial}{\partial x} \left(C_{11} \frac{\partial u_x}{\partial x} \right) - \beta^2 C_{44} u_x + i\beta \frac{\partial}{\partial x} (C_{12} u_y) + i\beta C_{44} \frac{\partial u_y}{\partial x} = -\omega^2 \rho u_x, \quad (68)$$

$$i\beta C_{12} \frac{\partial u_x}{\partial x} + i\beta \frac{\partial}{\partial x} (C_{44} u_x) + \frac{\partial}{\partial x} \left(C_{44} \frac{\partial u_y}{\partial x} \right) - \beta^2 C_{11} u_y = -\omega^2 \rho u_y, \quad (69)$$

where $\beta = k_1 + ik_2$ is the wave number along the y axis. The elastic constants C_{44} , C_{11} , and C_{12} are modified as dictated in Eqs. (49), (55), and (56) when the damping effect is included. Equations (68) and (69) are considered as an eigenvalue problem of determining the complex wave number β with given frequency ω . For a real group velocity v_g in the low-frequency limit $\omega \rightarrow 0$, we must have from Eq. (66) $(k_2/\omega)_{\omega=0} = (dk_2/d\omega)_{\omega=0} = 0$.

Now we consider the Pb/water system with and without damping to investigate the behaviors of the P-SH modes near the Γ point. In Fig. 4, we plot the real part k_1 and the imaginary part k_2 versus ω with decreasing filling ratio of water from (a) to (c). As the filling ratio is decreased, we see that the trends of imaginary parts of the P and SH modes are very different. For the SH mode without damping, the curve of k_1 versus ω is always tangent to the k_1 axis. In other words, $d\omega/dk_1 = 0$ at $\omega = 0$, which confirms the prediction from homogenization analysis: The group velocity of the SH mode is zero when incident angle $\theta = \pi/2$. If the damping effect is included, the imaginary part k_2 increases quickly as ω deviates from the Γ point. For the P mode, the curve of k_2 versus ω becomes flatter and flatter as the filling ratio of water is decreased. At a certain filling ratio, the curve is tangent to the ω axis, that is, $dk_2/d\omega = 0$, in the low-frequency limit $\omega \rightarrow 0$. In Fig. 5, we compute $dk_2/d\omega$ at $\omega = 0$ for four different systems: ice/water, Ag/water, C/water, and W/water. The filling ratios of water at which an evanescent mode becomes a propagating mode predicted by homogenization analysis and numerical computation are rather consistent with each other. In particular, the inset shows that $dk_2/d\omega = 0$ may become slightly negative between the critical filling ratio (of the solid material) and 1.

V. CONCLUDING REMARKS

In this study, we have developed a three-scale homogenization analysis to obtain the effective properties of periodic

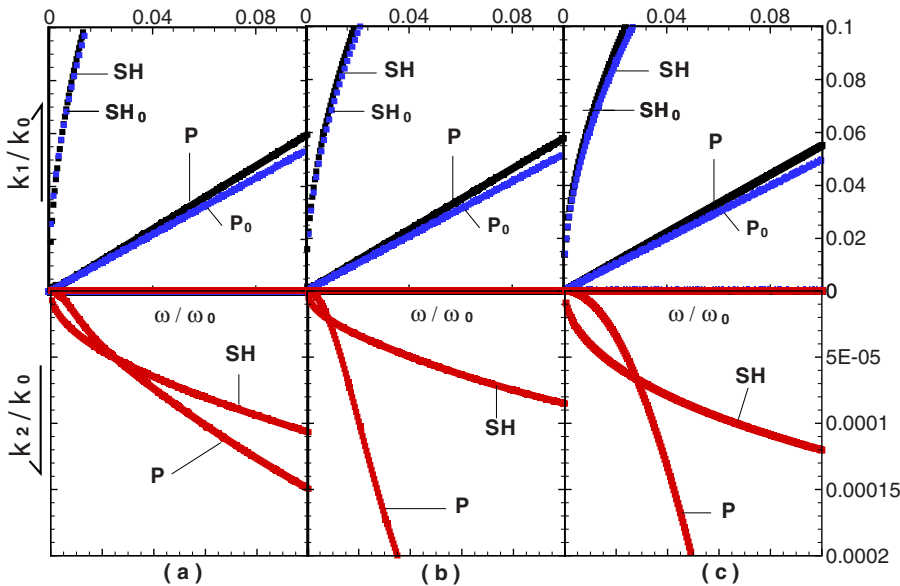


FIG. 4. (Color online) The behaviors of k_1 (black points) and k_2 (red points) at different filling ratios for the Pb/water system. The incident angle θ is $\pi/2$. The filling ratios of Pb are 0.5, 0.7, and 0.9 in (a), (b), and (c), respectively. It is noted that the frequency ω is normalized by $\omega_0 = \text{GHz}/\sqrt{2\pi}$ and k_1 and k_2 are normalized by $k_0 = \mu\text{m}/\sqrt{2\pi}$. In addition, P or SH with a subscript 0 (P_0 or SH_0) denotes the modes without damping effect.

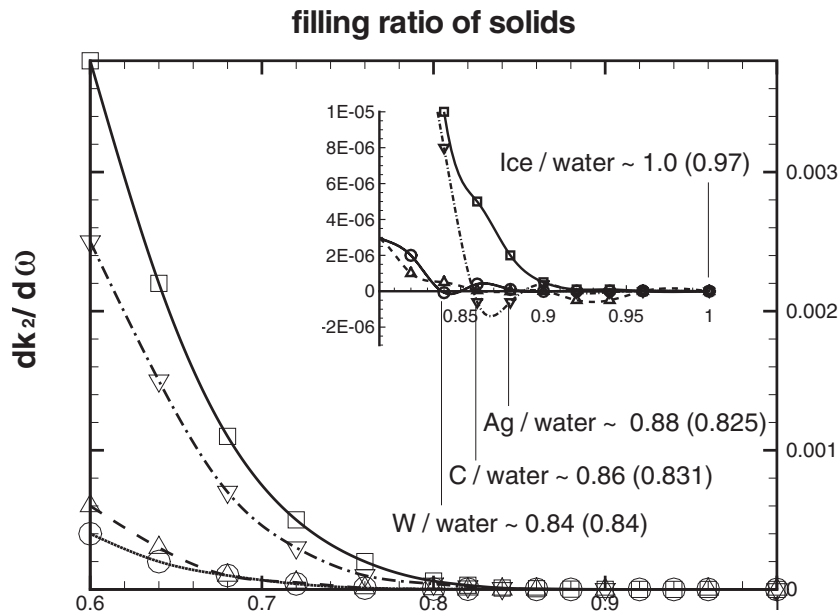


FIG. 5. The relation of $(dk_2/d\omega)_{\omega=0}$ versus the filling ratio of solid material for four composite systems: ice/water (solid line with squares), Ag/water (dashed line with triangles), C/water (dash-dotted line with deltas), and W/water (dotted line with circles). The inset on the upper right corner shows the details of the derivative versus the filling ratio of solid material between 0.8 and 1. The numerical values in the parentheses are obtained from homogenization analysis.

fluid-solid composite layers. The homogenized results were evaluated in the small ratio of the size of the periodic unit to the incident wavelength. First, we considered the case of ideal fluids then derived the explicit analytical formulas for the effective group velocities for the P and SH modes as well as the SV modes. It was shown that the effective-mass density is always the volume-averaged mass density of the solid and fluid phases, while the effective elastic constants are sophisticated combinations of individual elastic constants as well as the sinusoidal functions of the incident angle. Then, we investigated the case of viscous fluid, for which we have to consider complex Lamé constants for the fluid phase in the frequency-domain analysis. It was shown that the analytical forms for the effective group velocities remain the same but all the components must be modified by the effective viscosities which are six in number. It must be noted that the effective viscosities may also be influenced by the real elas-

tic constants of the solid and fluid, not just the viscosity of the fluid itself. In particular, we established a criterion under which $\langle \eta \rangle_{23}$ vanishes and thus propagating modes in the periodic solid-fluid layers are possible. These theoretical findings are supported by numerical simulations of the full elastic wave equations in the low-frequency limit. For future work, we will continue to investigate higher-dimensional problems and more complex material solid-fluid structures.

ACKNOWLEDGMENTS

The work was supported in part by the National Science Council of Taiwan under Contract Nos. NSC 96-2221-E-002-201 and NSC 97-2221-E-002-223-MY3 and by the Ministry of Economic Affairs of the Republic of China under Contract No. MOEA 94-EC-17-A-08-S1-0006.

*mechang@gate.sinica.edu.tw

- ¹J. E. White and F. A. Angona, *J. Acoust. Soc. Am.* **27**, 310 (1955).
- ²E. Behrens, *J. Acoust. Soc. Am.* **42**, 378 (1967).
- ³E. Behrens, *J. Acoust. Soc. Am.* **45**, 102 (1969).
- ⁴R. E. Camley, B. Djafari-Rouhani, L. Dobrzynski, and A. A. Maradudin, *Phys. Rev. B* **27**, 7318 (1983).
- ⁵B. Djafari-Rouhani, L. Dobrzynski, O. Hardouin Duparc, R. E. Camley, and A. A. Maradudin, *Phys. Rev. B* **28**, 1711 (1983).
- ⁶B. Djafari-Rouhani, A. A. Maradudin, and R. F. Wallis, *Phys. Rev. B* **29**, 6454 (1984).
- ⁷I. Cohen and David J. Bergman, *J. Mech. Phys. Solids* **51**, 1433 (2003).
- ⁸A. A. Krokhin, J. Arriaga, and L. N. Gumen, *Phys. Rev. Lett.* **91**, 264302 (2003).
- ⁹Q. Ni and J. Cheng, *Phys. Rev. B* **72**, 014305 (2005).
- ¹⁰Q. Ni and J. Cheng, *J. Appl. Phys.* **101**, 073515 (2007).
- ¹¹J. G. Berryman, *J. Acoust. Soc. Am.* **68**, 1809 (1980).
- ¹²J. G. Berryman, *J. Acoust. Soc. Am.* **68**, 1820 (1980).

- ¹³J. Mei, Z. Liu, W. Wen, and P. Sheng, *Phys. Rev. Lett.* **96**, 024301 (2006).
- ¹⁴R. Sprik and G. H. Wegdam, *Solid State Commun.* **106**, 77 (1998).
- ¹⁵X. Zhang, Z. Liu, J. Mei, and Y. Liu, *J. Phys.: Condens. Matter* **15**, 8207 (2003).
- ¹⁶Y. H. Liu, C. C. Chang, R. L. Chern, and C. C. Chang, *Phys. Rev. B* **75**, 054104 (2007).
- ¹⁷C. C. Mei, J.-L. Aurialt, and C. O. Ng, *Adv. Mech.* **32**, 277 (1996).
- ¹⁸J. Mei, Z. Liu, J. Shi, and D. Tian, *Phys. Rev. B* **67**, 245107 (2003).
- ¹⁹L. D. Landau and E. M. Lifshitz, *Theory of Elasticity, Course of Theoretical Physics*, 3rd ed. (Butterworth, Washington, DC/Heinemann, London, 1995), Vol. 7.
- ²⁰M. G. Cottam and D. R. Tilley, *Introduction to Surface and Superlattice Excitations* (Cambridge University Press, New York, 1989).